ELSEVIER

Journal of Photochemistry and Photobiology A: Chemistry 102 (1996) 59–70

Journal of PHOTOCHEMISTRY AND PHOTOBIOLOGY A:CHEMISTRY

Intramolecular charge transfer in the excited state. Kinetics and configurational changes

K.A. Zachariasse, M. Grobys, Th. von der Haar, A. Hebecker, Yu.V. Il'ichev, Y.-B. Jiang, O. Morawski, W. Kühnle

Max-Planck-Insitut für biophysikalische Chemie, Spektroskopie und Photochemische Kinetik, Postfach 2841, D-37018 Göttingen, Germany

Abstract

The fast excited state intramolecular charge transfer (ICT) and dual fluorescence observed with several 4-aminobenzonitriles is discussed. The magnitude of the energy gap between the two lowest excited states is shown to determine the occurrence or absence of ICT. The excited state behaviour of a series of six 4-aminobenzonitriles in which the amino nitrogen atom is part of a three- to eight-membered heterocyclic ring, P3C to P8C, is studied by using photostationary and time-resolved fluorescence measurements. The ICT rate constant strongly decreases with decreasing ring size. ICT does not occur with P3C and P4C in diethyl ether. This is attributed to the increase of the amino nitrogen inversion barrier with decreasing ring size. The configurational change of the amino nitrogen from pyramidal to planar is considered to be an important reaction coordinate in the ICT process. The photophysics of the 4-aminobenzonitriles is different from that of other systems such as donor/acceptor-substituted stilbenes and 9,9'-bianthryl, which are governed by the charge distribution and macroscopic Coulombic interaction in their CT states.

Keywords: Intramolecular charge transfer; Photostationary fluorescence; Time-resolved fluorescence; Aminobenzonitriles

1. Introduction

With 4-(dimethylamino)benzonitrile (DMABN) and related electron donor/acceptor (D/A)-substituted benzenes dual fluorescence is observed in sufficiently polar solvents (more polar than alkanes), which originates from fast intramolecular charge transfer (ICT) [1–3]. During the ICT process the molecular dipole moment μ increases, from 6.6 D in the ground state to 9–10 D in the initially prepared locally excited (LE) state and then finally to around 16 D in the equilibrated CT state [4]. The increase in dipole moment takes place in two relatively small steps of 3 D ($S_0 \rightarrow$ LE) and 6–7 D (LE $\rightarrow$ CT). The substantial value of 16 D for μ(CT) should be seen in relation to the largest possible dipole moment of around 33 D for the hypothetical planar quinoidal resonance structure of DMABN [1]. Similarly, for trans-4-dimethylamino-4'-cyano-stilbene (DCS) (see below) a dipole moment of 65 D can in principle be reached, which should be compared with the measured μ(CT) of 22 D[1] [6].

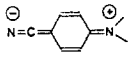
DMABN (33 D)

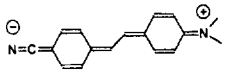
DCS (65 D)

The dual fluorescence coupled with ICT as observed with DMABN has attracted considerable attention since its discovery in 1959 [7]. A large variety of mechanisms has been presented in the literature to explain this phenomenon [2]. Among these, the model of "Twisted Internal Charge Transfer" (TICT) pioneered by Grabowski [1,8](a), has played a prominent role. According to this model, the dimethylamino and benzonitrile groups in the CT state of DMABN are in a mutually perpendicular configuration, which is assumed to lead to complete electronic decoupling. It has recently been shown, however, that in the CT state of a dual fluorescent aminobenzonitrile the amino group is strongly coupled to the

[1] The dipole moment of 33 D for the quinoidal CT state of DMABN is derived from a distance of 6.9 Å between the nitrogen atoms of the amino and cyano group of DMABN, as determined by PCMODEL [5]. A distance of 13.6 Å between these nitrogens in DCS is used in the calculation of the value of 65 D for the planar quinoidal resonance structure. An LE precursor state of DCS has not been observed with certainty (see text) and hence its dipole moment is not known.

[2] The following mechanisms for the ICT reaction of DMABN and related molecules were proposed in the literature: (a) state inversion (^1L_b,^1L_a) [7]; (b) rotational isomerisation and decoupling of the amino group (TICT) [1,8](a); (c) excimer/dimer [8](b); (d) protonation (deuteration effect), [8](c); (e) 1:1 solute/solvent exciplex [8](d); and (f) reaction with ubiquitous water molecules [8](e).

PII S1010-6030(96)04368-7

rest of the molecule, which leads to the assumption that the CT state has a planar configuration [9].

ICT in the excited state also takes place in a variety of other molecules besides the aminobenzonitriles. Here, D/A-substituted naphthalenes, bianthryls and D/A-substituted stilbenes are discussed in connection with the ICT reaction mechanism deduced for the aminobenzonitriles. In all these systems, except the stilbenes, dual emission from an LE state and a CT state is already observed in the photostationary fluorescence spectra. The CT state is formed only from the primarily prepared LE state. The presence of an LE precursor in the ICT reaction occurring with D/A-stilbenes is still a point of discussion [6](b).

In the following, the molecular electronic and configurational factors controlling the ICT reaction in aminobenzonitriles are discussed. It is shown that the energy gap $\Delta E(S_1,S_2)$ between the two lowest singlet excited states and the level ordering of the S_1 and S_2 states determines the occurrence of such a reaction. A second important factor is the energetics of the change in configuration of the amino nitrogen from a (partly) pyramidal (sp^3) towards a planar (sp^2) hybridisation. This change was deduced from experiments with a series of heterocyclic aminobenzonitriles as a function of the ring size of the amino group. Further, the flexibility of the amino nitrogen as well as the influence of the (rotor) size and of the electron donor and acceptor properties of the D and A subunits of the aminobenzonitriles on the ICT reaction and the fluorescence spectra is treated.

In a treatment of the ICT reaction in bianthryls, D/A-stilbenes and D/A-naphthalenes the generality of the mechanism deduced for the aminobenzonitriles is discussed.

2. Experimental section

The synthesis of the compounds discussed here has been described previously [3,4] or will be reported separately. The following abbreviations are used (Fig. 9(a)): CBQ, 6-cyanobenzoquinuclidine; DEABN, 4-(diethylamino)-benzonitrile; DMABN, 4-(dimethylamino)benzonitrile; EDB, 4-(*N,N*-diethylamino)-2,6-dimethyl-benzonitrile; MDB, 4-(*N,N*-dimethylamino)-2,6-dimethyl-benzonitrile; MMD, 4-(*N,N*-dimethylamino)-3,5-dimethyl-benzonitrile; P5C, 4-(*N*-pyrrolidinyl)benzonitrile; P6C, 4-(*N*-piperidinyl)benzonitrile; P6N, *N*-(4-cyanophenyl)-*N'*-methylpiperazine; P6O, 4-(*N*-morpholinyl)benzonitrile; P7C, 4-(*N*-hexahydroazepinyl)benzonitrile; P8C, 4-(*N*-octahydroazocinyl)benzonitrile; PDB, 4-(*N,N*-di-n-propylamino)-2,6-dimethylbenzonitrile.

The fluorescence spectra were measured by using a quantum-corrected Shimadzu 5000PC spectrophotometer. The picosecond time-correlated single-photon counting (SPC) data were obtained with a system described previously [3,4] and (see Fig. 1) with a picosecond system consisting of a mode-locked Titanium-sapphire laser (Coherent, MIRA 900-F) pumped by an argon ion laser (Coherent, Innova 415).

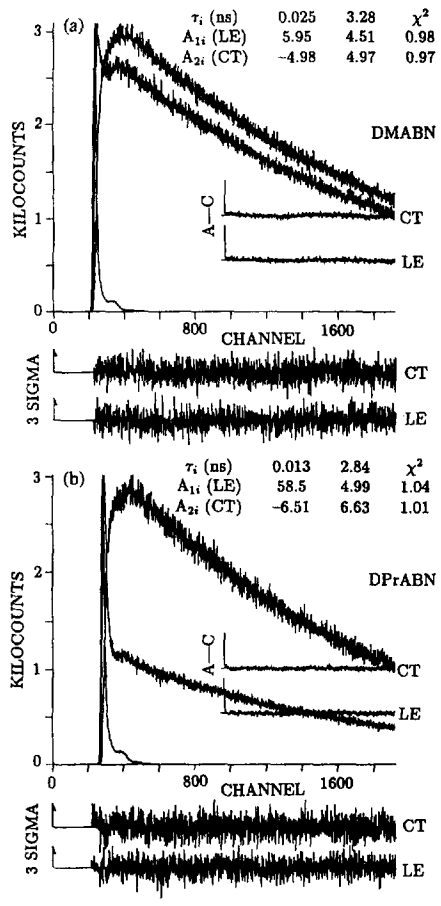

Fig. 1. Fluorescence response functions of the LE and CT emission of (a) 4-(dimethylamino)benzonitrile (DMABN) and (b) 4-(di-n-propylamino)benzonitrile (DPrABN) in diethyl ether at 20 °C. The decay times (τ_2, τ_1) and their preexponential factors A_{2i} (CT) and A_{1i} (LE) are given. The LE and CT decays were analyzed simultaneously (global analysis [10]). The decays were obtained by using picosecond laser excitation at 296 nm. The weighted deviations, expressed as σ (expected deviations) and the autocorrelation functions *A–C* are indicated.

The analysis of the fluorescence decays was carried out by using the method of modulating functions [3] [10].

3. Charge transfer and dual fluorescence

3.1. Reversible fast charge transfer. CT state reached from LE precursor

DMABN in diethyl ether at 20 °C undergoes a fast reversible ICT reaction upon excitation. This is seen (Fig. 1(a)) from the double-exponential LE fluorescence decay $i(\leq) = A_{12}e^{-t/\tau_2} + A_{11}e^{-t/\tau_1}$ with time constants $\tau_2 = 25$ ps and $\tau_1 = 3.28$ ns and a ratio $A = A_{12}/A_{11}$ of 1.3, obtained by global analysis of the SPC data[3] [10]. The preexponential

[3] When $\tau_2 \ll \tau_1$, as in Fig. 1, the rate constants of the forward (k_a) and backward (k_d) ICT reactions can be determined in an approximate manner from $k_a + k_d \simeq 1/\tau_2$ and $k_a/k_d = A_{12}/A_{11}$. Using this procedure in the case of DMABN (Fig. 1(a)) the values $k_a = 2.28 \times 10^{10}$ s^{-1} and $k_d = 1.72 \times 10^9$ s^{-1} result, in good agreement with the outcome of a full analysis, with $\tau_0 = 3.91$ ns at diethyl ether at 20 °C from MABN as the model compound (cf. Ref. [3]): 2.26×10^{10} s^{-1} (k_a) and 1.71×10^9 s^{-1} (k_d).

Scheme 1.

factors A_{2i} of the CT fluorescence rise and decay curve $i(\mathrm{CT}) = A_{22}e^{-t/\tau_2} + A_{21}e^{-t/\tau_1}$ are practically equal and of opposite sign (Fig. 1), which means that the concentration of the CT state at $t = 0$ is equal to zero, i.e. the CT state is not produced by direct excitation of the ground state [3]. A similar situation is observed with 4-(di-n-propylamino)benzonitrile (DPrABN) (see Fig. 1(b)).

Therefore, ICT can be described with Scheme 1 where, besides the forward (k_a) and backward (k_d) reaction rate constants, also the (reciprocal) lifetimes of the LE ($1/\tau_o$) and the CT ($1/\tau_o'$) states are indicated.

From the decay times τ_2 and τ_1 together with the amplitude ratio $A = A_{12}/A_{11}$ of the LE decay (Fig. 1) the following values are calculated[3] [3]: $k_a = 2.3 \times 10^{10}\ \mathrm{s}^{-1}$, $k_d = 1.7 \times 10^{10}\ \mathrm{s}^{-1}$ (DMABN, Fig. 1(a)) and $k_a = 7.1 \times 10^{10}\ \mathrm{s}^{-1}$, $k_d = 6.0 \times 10^{9}\ \mathrm{s}^{-1}$ (DPrABN, Fig. 1(b)). It is seen from these data that upon increasing the length of the amino alkyl groups the ICT rate constant k_a becomes larger and the thermal back reaction k_d becomes slower [4,11]. A still faster ICT reaction is observed with 4-azetidinyl-3,5-dimethylbenzonitrile (M4D) in diethyl ether at 20 °C. From $\tau_2 = 2$ ps, $\tau_1 = 711$ ps and a ratio A_{12}/A_{11} of 1 600 it follows that $k_a = 5 \times 10^{11}\ \mathrm{s}^{-1}$ and $k_d = 3 \times 10^{8}\ \mathrm{s}^{-1}$: a nearly irreversible reaction[3] [12].

3.2. CT Stokes shift due to ground state repulsion

The activation energies of the forward (E_a) and backward (E_d) ICT reactions (Scheme 1) can be determined by measuring the LE and CT fluorescence decays as a function of temperature. For DMABN in diethyl ether the following results are obtained: $E_a = 4.0$ kJ mol^{-1} and $E_d = 20.6$ kJ mol^{-1}, giving a stabilisation enthalpy $-\Delta H (= E_a - E_d)$ of 17 kJ mol^{-1} [13,14]. Using these data together with the CT emission maximum $h\nu^{\max}(\mathrm{CT})$ of 23 850 cm^{-1} (20 °C) and the energy difference $\Delta E(\mathrm{LE})$ between the LE and the ground state (31 300 cm^{-1}),[1] the energy of the CT Franck–Condon ground state $\delta E_{rep} = 73$ kJ mol^{-1} is obtained (Eq. (1)). A similar result ($-\Delta H = 10$ kJ mol^{-1} and $\delta E_{rep} = 75$ kJ mol^{-1}) is found with DMABN in toluene [11].

$$\delta E_{rep} = \Delta E(\mathrm{LE}) - (-\Delta H) - h\nu^{\max}(\mathrm{CT}) \quad (1)$$

It clearly follows from a comparison of the values for $-\Delta H$ and δE_{rep} that the large Stokes shift (cf. Fig. 4) of the CT emission of DMABN in diethyl ether is due for the most part to the fact that the Franck–Condon state reached upon CT emission has a considerably higher energy (δE_{rep}) than the equilibrated ground state S_0. It is precisely this situation, generally encountered in dual fluorescent aminobenzonitriles [3,4,9] which makes the spectral separation of the LE and CT emission possible. Under the condition of small values for $-\Delta H$ and δE_{rep} it would otherwise be difficult to decide whether a dual emission from LE and CT is present, such as with 9,9′-bianthryl in n-hexane (see below) [15].

4. Absence of dual fluorescence

4.1. Importance of the energy gap $\Delta E(S_1,S_2)$

In contrast to DMABN, an excited state charge transfer reaction accompanied with dual fluorescence is not observed in the case of the two dimethylaminobenzonitriles having the dimethylamino group in the ortho or the meta position: o-DMABN and m-DMABN. This is the case even in a polar solvent such as acetonitrile, in which the measured fluorescence decays are single exponential [16].

Similarly, dual fluorescence is absent irrespective of solvent polarity or temperature when one or both methyl groups of the dimethylamino substituent are replaced by hydrogen: 4-(methylamino)benzonitrile (MABN) and 4-aminobenzonitrile (ABN) [3,4,16]. From the absorption spectra of these molecules it is seen that the two lowest singlet excited states $S_1(L_b)$ and $S_2(L_a,\mathrm{CT})$ have a larger energy gap than that present in DMABN and the other aminobenzonitriles showing dual fluorescence [11,16].

The absence of dual fluorescence with MABN is not due to the decreased donor strength ($\simeq 0.3$ eV, Ref. [3]) of the methylamino as compared with the dimethylamino group, which negative effect on ΔG can easlily be overcome by increasing the solvent polarity. The difference in free energy involved in the ICT reaction from LE to a CT state of 16 D amounts to 0.8 eV when going from n-hexane to acetonitrile [3]. This estimate is fully supported by the difference in the energy of the CT emission maxima in n-hexane and acetonitrile, which has a value of 0.66 eV for DMABN. Moreover, the difference of 0.1 eV between the S_1 energies of MABN and DMABN would lead, within the context of the TICT hypothesis [1,2], to an increase of $-\Delta G$ by this amount.

Dual fluorescence is observed with 4-(methylamino)-3,5-dimethylbenzonitrile (MHD) in slightly polar (diethyl ether) and polar (acetonitrile) solvents [16]. The lack of dual fluorescence in the case of MABN can therefore not be attributed to an intrinsic property of the methylamino group. From the absorption spectra of MHD it is seen that the energy gap $\Delta E(S_1,S_2)$, which in n-hexane is comparable to that of DMABN and hence prevents ICT, likewise becomes sufficiently small for the occurrence of an ICT reaction in more polar solvents [16].

5. The energy gap $\Delta E(S_1,S_2)$ and dual fluorescence

5.1. Dicyanoanilines

The fluorescence spectra of 3,4-dicyano-*N*,*N*-dimethylaniline (3,4-DCDMA) and 3,5-dicyano-*N*,*N*-dimethylaniline(3,5-DCDMA) exclusively consist of an aniline-like LE emission, in unpolar as well as in polar solvents irrespective

of temperature [9,16]. It is therefore concluded that ICT does not occur with these dicyanoanilines. This conclusion is supported by the single-exponential character of the picosecond fluorescence decays of 3,5-DCDMA in acetonitrile [16] and of 3,4-DCDMA and 3,5-DCDMA in diethyl ether at 25 °C as well as at lower temperatures [9]. DMABN, under such conditions, undergoes an efficient ICT reaction (Fig. 1(a)).

The observed absence of ICT and dual fluorescence can again be correlated with the magnitude of the energy gap $\Delta E(S_1,S_2)$, which for 3,4-DCDMA and 3,5-DCDMA is considerably larger than for the 4-aminobenzonitriles. This increase in $\Delta E(S_1,S_2)$ is due to the asymmetric substitution pattern in the dicyano compounds, which leads to an extensive mixing of the ^1L_a and ^1L_b states of the parent benzene system. The character of these states in unsubstituted benzene is determined by the symmetry of its molecular orbitals, which is destroyed by substituents, especially in the ortho and meta positions [17].

The finding that these dicyanoanilines do not show dual fluorescence contrary to DMABN is surprising within the context of the TICT model. In this model, the energetics of the CT state is thought to be determined by the redox potentials of the amino (D) and dicyanobenzene (A) subunits, and dicyanobenzene is a considerably better electron acceptor than benzonitrile [9].

5.2. *Energy reversal of the two lowest excited states $S_1(^1L_a,CT)$ and $S_2(^1L_b)$*

In the aminobenzonitriles discussed until now the more strongly allowed (^1L_a,CT) state has a higher energy than the ^1L_b state. This level ordering can be reversed, as in M4D, 4-(dimethylamino)-3,5-dimethylbenzonitrile (MMD) and 6-cyanobenzoquinuclidine (CBQ) [18–20]. Dual fluorescence is observed in the case of M4D, with an ICT rate constant k_a considerably larger than that of DMABN or DEABN, as shown above. In MMD, having a larger energy gap between $S_1(^1L_a,CT)$ and $S_2(^1L_b)$ than M4D, the width of the fluorescence band (mainly CT) is clearly larger in n-pentane than in the more polar solvents toluene and acetonitrile [16]. This difference in bandwidth has been attributed to the presence of an LE component in the photostationary emission spectrum of MMD in n-pentane, whereas it is assumed that in toluene and acetonitrile only a CT emission can be observed [16]. The fluorescence decays of MMD in n-pentane, however, are single exponential within the time resolution (5–10 ps) of the SPC equipment. On the basis of these measurements it can therefore not be decided with certainty, whether or not dual fluorescence occurs with MMD [4].

[4] The fact that with MMD, in contrast to DMABN, ICT is observed in a supersonic jet [21], can be understood on the basis of the energy reversal of ^1L_b and (^1L_a,CT) in the two molecules (see Fig. 3).

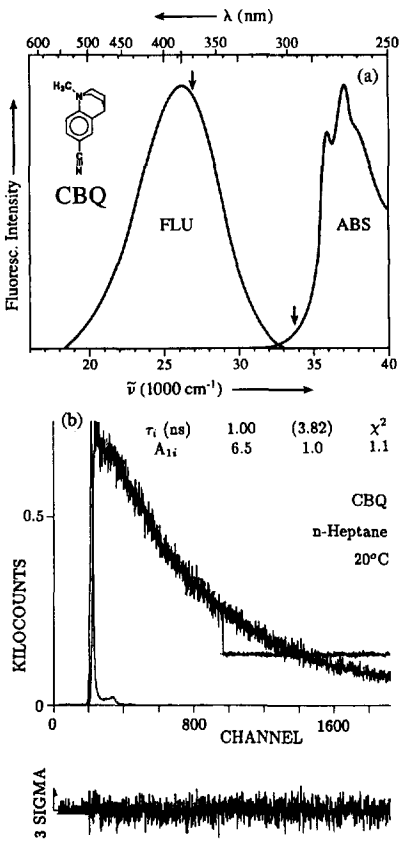

Fig. 2. (a) Fluorescence and absorption spectra of 6-cyanobenzoquinuclidine (CBQ) in n-hexane at 20 °C and (b) LE fluorescence response functions of CBQ in n-heptane at 20 °C. See the caption of Fig. 1.

5.2.1. *6-Cyanobenzoquinuclidine*

In the case of 6-cyanobenzoquinuclidine (CBQ) the fluorescence spectrum consists of a broad emission band (Fig. 2(a)): there is no sign of dual fluorescence in solvents of different polarity over a large temperature range. In accordance with this conclusion, the fluorescence decay of CBQ in n-heptane at 20 °C is single exponential (Fig. 2(b)) and does not contain the fast component τ_2 which is normally present when ICT occurs.

The main band in the absorption spectrum of CBQ (Fig. 2(a)) is similar to that of 4-methylbenzonitrile [20]. The low-energy part of the CBQ spectrum has been attributed to the weak (^1L_a,CT) band, which means that a state reversal has occurred as compared to DMABN. Hence, excitation at 296 nm directly populates the (^1L_a,CT) state, from which the fluorescence then originates: the normal situation encountered in the majority of fluorescing molecules. With CBQ the energy gap between $S_1(^1L_a,CT)$ and $S_2(^1L_b)$ is still larger than with MMD or M4D, which apparently precludes the occurrence of dual fluorescence (Fig. 2(a)).

5.3. *Level ordering of the (^1L_a,CT) and ^1L_b states. Energy gap $\Delta E(S_1,S_2)$ and vibronic interaction*

It follows from the preceding sections that the occurrence of dual fluorescence in aminobenzonitriles can be understood

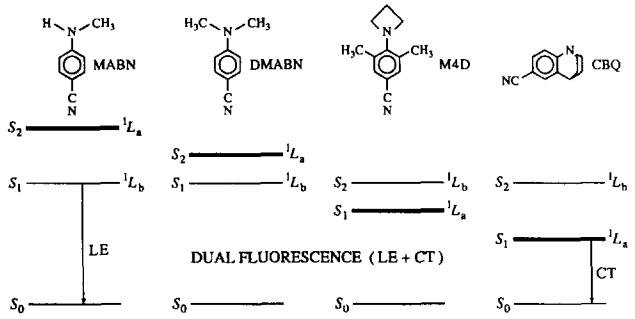

Fig. 3. Different level ordering of the two lowest excited states ^1L_b and (^1L_a,CT) for 4-aminobenzonitriles.

on the basis of the magnitude of the energy gap $\Delta E(S_1,S_2)$. Dual fluorescence and an LE → CT reaction is observed when the energy gap $\Delta E(S_1,S_2)$ is sufficiently small for the onset of vibronic coupling, leading to a solvent-induced pseudo-Jahn–Teller interaction [9,16,22]. Two cases are encountered (Fig. 3): ^1L_b below (^1L_a,CT) with DMABN as an example, and (^1L_a,CT) lower than ^1L_b, which occurs in the case of M4D and, possibly (see above), MMD [16,22,23].

Dual fluorescence does not occur when $\Delta E(S_1,S_2)$ is too large for effective vibronic coupling between S_1 and S_2, such as with MABN ($S_1(^1L_b)$) and CBQ ($S_1(^1L_a$, CT)). In these cases normal fluorescence from a single excited state is observed: LE for MABN and CT for CBQ [9,16,20,22].

5.4. *Influence of the size of the D and A subgroups on ICT*

In order to investigate the influence of the size of the amino (D) and benzonitrile (A) subgroups on the ICT reaction, a series of 4-(dialkylamino)benzonitriles and 4-(dialkylamino)-2,6-dimethylbenzonitriles were investigated.

5.4.1. *4-(Dialkylamino)benzonitriles*

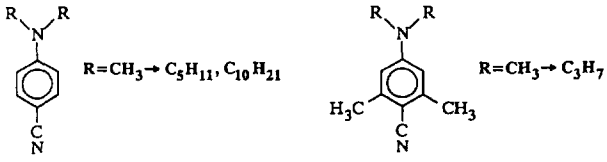

In a series of 4-(dialkylamino)benzonitriles in which the alkyl groups increase in length from methyl to decyl the CT/LE fluorescence quantum yield ratio $\Phi'(CT)/\Phi(LE)$, and hence the ICT efficiency, increases with the length of the alkyl substituents. Whereas with DMABN in the non-polar solvent cyclohexane hardly any CT emission is present, the other 4-(dialkylamino)benzonitriles (ethyl (DEABN), propyl (DPrABN), decyl (DDABN)) clearly show dual fluorescence [4,11]. These first examples of dual emission of aminobenzonitriles in alkane solvents show that a polar solvent is not an essential requirement for the ICT reaction. Also in more polarisable and polar solvents such as benzene [4], toluene (DMABN, DEABN and DPrABN) (see Fig. 4) and 1,4-dioxane [4] an increase of $\Phi'(CT)/\Phi(LE)$ with chain length is observed. As discussed above (Fig. 1), the ICT rate constant k_a in diethyl ether at 20 °C of DPrABN is about three times larger than that of DMABN.

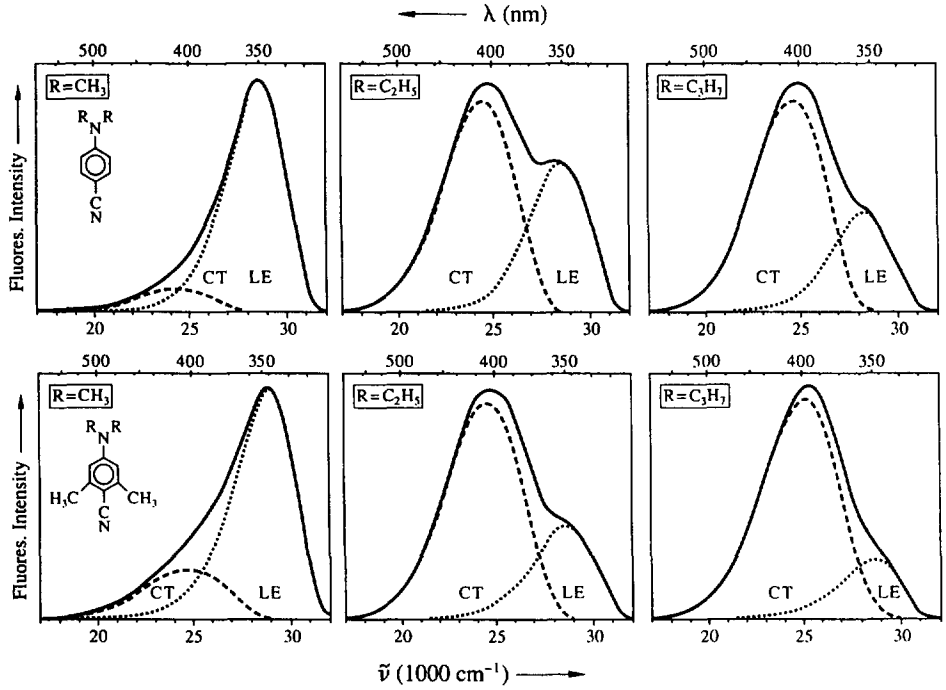

Fig. 4. Fluorescence spectra of (top) the 4-(dialkylamino)benzonitriles DMABN (methyl), DEABN (ethyl) and DPrABN (n-propyl) and (bottom) the 4-(dialkylamino)-2,6-dimethylbenzonitriles MDB (methyl), EDB (ethyl) and PrDB (n-propyl) in toluene at 25 °C. The CT and LE emission bands are separated by taking the shape of the spectrum of 4-(methylamino)benzonitrile (MABN) for the LE state.

5.4.2. 4-(Dialkylamino)-2,6-dimethylbenzonitriles

Similarly, $\Phi'(CT)/\Phi(LE)$ increases upon enlarging the size of the benzonitrile moiety by two methyls next to the cyano group, which is seen by comparing the spectra of the two series of aminobenzonitriles in Fig. 4 [9,11]. For the 4-(dialkylamino)-2,6-dimethylbenzonitriles (methyl (MDB), ethyl (EDB) and propyl (PDB)) the relative importance of the CT emission again increases with alkyl chain length.

The observation that the ICT reaction in 4-aminobenzonitriles becomes more efficient upon increasing the size of the amino as well as the benzonitrile subgroups goes contrary to what is to be expected when a rotational isomerisation of the amino group from planar to perpendicular would take place as required in the TICT model. Similar results have been obtained with a series of ethyl esters of 4-(dialkylamino)benzoic acids [23,24].

The introduction of the two additional methyl groups in the 4-(dialkylamino)-2,6-dimethylbenzonitriles leads to a reduction of the $\Delta E(S_1,S_2)$ energy gap, as seen from their absorption spectra. The lengthening of the alkyl groups of the amino substituent causes a reduction of the inversion barrier of the amino nitrogen [5] [25,26]. Both factors, the energy gap between S_1 and S_2 as well as the energy involved in a change in the configuration of the amino nitrogen from pyramidal towards planar, have been shown in the previous sections to play an important role in controlling the ICT reaction of aminobenzonitriles.

The increase in ICT efficiency with the size of the amino substituent described here is not due to an increase in the electron donor strength when going from a dimethylamino to a decylamino group, contrary to what has been suggested [27]. This follows from the absence of a correlation between the redox potentials of the D and A subunits of a group of aminobenzonitriles and their CT emission maxima [9]. Furthermore, the presence of the two additional methyl groups in MDB–PDB reduces the electron affinity of the benzonitrile moiety relative to that in DMABN–DPrABN, as seen from the reduction potentials [28] for benzonitrile (−2.34 V vs. SCE) and 2,4,6-trimethylbenzonitrile (−2.47 V vs. SCE).

6. Flexibility of the amino nitrogen

The aminobenzonitrile 1-methyl-7-cyano-2,3,4,5-tetrahydro-1H-1-benzazepine (NMCB) in which the amino nitrogen is connected to the phenyl ring by a tetramethylene chain, undergoes ICT and shows dual fluorescence [11,16]. This is seen from the fluorescence spectrum of NMCB in diethyl ether at −110 °C, as an example, which consists of a CT emission band next to a minor LE band (Fig. 5).

In contrast to the seven-membered heterocyclic molecule NMCB, the fluorescence spectra of the related molecules with six- and five-membered rings (1-methyl-5-cyanoindoline (NMCI) and 1-methyl-6-cyano-1,2,3,4-tetrahydroquinoline (NMCQ)) only consist of an LE emission band. No indication of the appearance of dual fluorescence is found with these molecules in a large variety of polar and non-polar solvents as a function of temperature [1–3]. This conclusion is supported by recent solvatochromic measurements with NMCQ and NMCB [20].

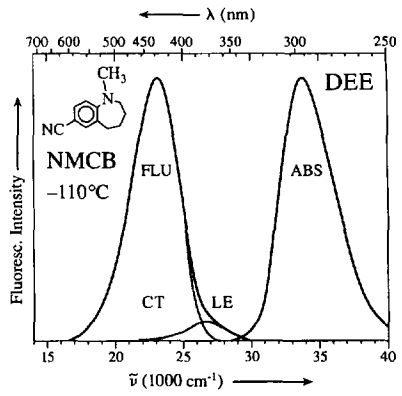

Fig. 5. Fluorescence spectrum of 1-methyl-7-cyano-2,3,4,5-tetrahydro-1H-1-benzazepine (NMCB) in diethyl ether at -110 °C. See the caption of Fig. 4.

The occurrence of efficient ICT with NMCB is attributed to the increased flexibility of the amino nitrogen in its seven-membered heterocyclic unit as compared to the more rigid NMCI and NMCQ molecules. This means that the possibility to reach a mutually perpendicular configuration of the amino group and the phenyl ring clearly is not a requirement for the appearance of ICT and dual fluorescence, contrary to the TICT model.

7. Heterocyclic aminobenzonitriles

7.1. Influence of ring size on ICT with heterocyclic aminobenzonitriles

In the series of 4-aminobenzonitriles P8C (*N*-octahydroazocinyl), P7C (*N*-hexahydroazepinyl), P6C (*N*-piperidinyl), P5C (*N*-pyrrolidinyl), P4C (*N*-azetidinyl) and P3C (*N*-aziridinyl), in which the amino nitrogen is incorporated in a heterocyclic ring, the quantum yield ratio $\Phi'(CT)/\Phi(LE)$ and the ICT rate constant k_a strongly decrease with decreasing ring size [9,22].

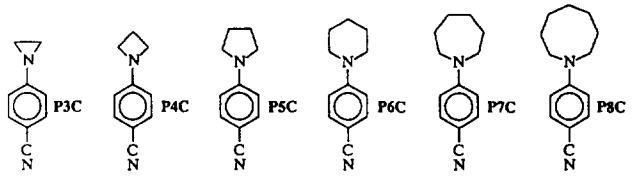

The fluorescence spectrum of P8C in diethyl ether at 20 °C mainly consists of a CT emission, with $\Phi'/\Phi = 2.8$. This ratio Φ'/Φ strongly decreases with ring size in the series P8C → P3C [9,11,22]. With P4C and P3C in diethyl ether dual fluorescence cannot be detected: an ICT reaction does not take place. A CT emission is not even found at low temperatures, a condition favourable for its observation, as

[5] This follows from preliminary picosecond fluorescence data showing that the relaxation of the amino group from pyramidal to planar is faster for *N,N*-dibutylaniline than for *N,N*-dimethylaniline (Ref. [12]).

Φ'/Φ increases with decreasing temperature when the CT stabilisation enthalpy ΔH is small and the thermal back reaction k_d (Scheme 1) consequently large [3].

The occurrence of ICT for P8C-P5C and its absence for P4C and P3C in diethyl ether can also be deduced from the LE fluorescence decays at −80 °C, for example, which are double exponential for P8C-P5C, but single exponential for P4C and P3C [20,22]. From an analysis of the decay times τ_1 and τ_2 together with the LE amplitude ratio A, it follows that under these conditions the ICT rate constant k_a is an order of magnitude larger for P6C (11.9×10^9 s^{-1}) than for P5C (1.1×10^9 s^{-1}) [22]. At 20 °C in diethyl ether, the following values for k_a are determined [16,25] from the double-exponential LE fluorescence decays: 63×10^9 s^{-1} (P7C), 43×10^9 s^{-1} (P6C) and 5×10^9 s^{-1} (P5C) [16]. Clearly, not only Φ'/Φ but also the rate constant k_a decreases with ring size in the series PnC. The higher ICT efficiency of P6C as compared to P5C has been found before in several solvents at low temperatures [29].

A similar dependence of the ICT reaction efficiency on the size of the amino ring is observed for P8C–P3C in the polar solvent acetonitrile. Here, $\Phi'(CT)/\Phi(LE)$ at 20 °C decreases from around 25 (P8C) to zero (P3C). Different from diethyl ether, however, P4C shows dual fluorescence in acetonitrile: $\Phi'/\Phi=0.41$ (Fig. 6). Note that the CT emission maxima $h\nu^{max}$(CT) occur at approximately the same energy. This insensitivity of $h\nu^{max}$(CT) to molecular structure is generally encountered with dual fluorescent 4-aminobenzonitriles. It indicates that the amino and benzonitrile subgroups in the ICT state are strongly coupled (see below) [9].

From the fluorescence decay times τ_1 and τ_2 together with their amplitude ratio A as a function of temperature, an Arrhenius plot of the rate constants k_a and k_d and the reciprocal CT lifetime ($1/\tau'_o$) can be constructed. Such plots are presented in Fig. 7 for P4C and P5C in acetonitrile, giving the activation energies E_a (13.5 kJ mol^{-1} (P4C); 8.0 kJ mol^{-1} (P5C)) and E_d (28.9 kJ mol^{-1} (P4C); 24.2 kJ mol^{-1} (P5C)) of the forward and backward ICT reaction. Using these data, the CT stabilisation enthalpy ($-\Delta H=15.4$ kJ mol^{-1} (P4C); 16.2 kJ mol^{-1} (P5C)) can be calculated. Similar experiments

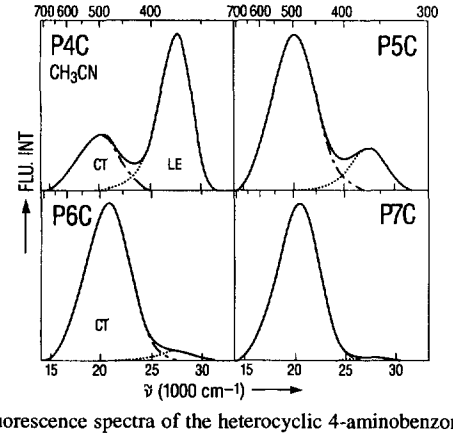

Fig. 6. Fluorescence spectra of the heterocyclic 4-aminobenzonitriles P4C (azetidinyl), P5C (pyrrolidinyl), P6C (piperidinyl), and P7C (hexahydroazepinyl) in acetonitrile at 20 °C. See the caption of Fig. 4.

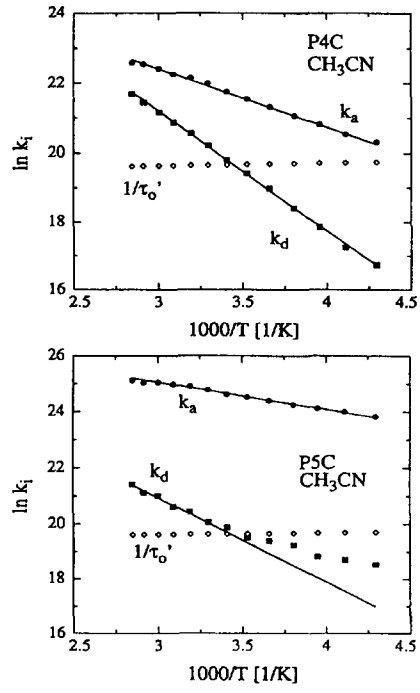

Fig. 7. Arrhenius plots of the reaction parameters k_a, k_d and $1/\tau_o'$ (Scheme 1) for (top) 4-(*N*-azetidinyl)benzonitrile (P4C) and (bottom) 4-(*N*-pyrrolidinyl)benzonitrile (P5C) in acetonitrile.

have been carried out for P6C and P7C [11,13] (see Table 1).

It is seen from this table that in acetonitrile the activation energy E_a of the ICT reaction clearly increases with decreasing ring size from P7C (4.7 kJ mol^{-1}) to P4C (13.5 kJ mol^{-1}). A similar trend is observed for P7C to P5C in diethyl ether (see Table 1) [13]. These data show that the increase in the activation energy is the reason for the decrease in ICT efficiency in the series P7C to P4C. Note that the ICT reaction enthalpy $-\Delta H$ for the PnC molecules in acetonitrile and in diethyl ether is practically independent of the ring size n (Table 1), which means that the molecular nature of the ICT product state is not a rate determining factor.

From the temperature dependence of the rate constants of the forward (k_a) and backward (k_d) reactions it is concluded that the ICT with 4-aminobenzonitriles such as DMABN and the PnC compounds is not a barrierless process, contrary to assumptions made in the literature [2].

Table 1
Shortest decay time τ_2 and thermodynamic parameters E_a and $-\Delta H$ for the ICT reaction with the aminobenzonitriles P4C–P7C (see Scheme 1 and text) in acetonitrile and diethyl ether (DEE)

			P4C	P5C	P6C	P7C
τ_2 [a]	(CH_3CN)	(ps)	266	19	6	5
E_a	(CH_3CN)	(kJ mol^{-1})	13.5	8.0	6.6	4.7
$-\Delta H$	(CH_3CN)	(kJ mol^{-1})	15	16	–	–
E_a	(DEE)	(kJ mol^{-1})	–[b]	7.2	6.0	(6.9)
$-\Delta H$	(DEE)	(kJ mol^{-1})	–	13	13	14

[a] At 20 °C.
[b] With P4C in diethyl ether an ICT reaction does not take place.

Table 2
Data for the amino nitrogen inversion barrier $\Delta G^{\ddagger}$ derived from dynamic NMR spectroscopy [26]

		M3N [a]	M4N [a]	M5N [a]	M6N [a]	M7N [a]
$\Delta G^{\ddagger}$	(kJ mol^{-1})	79.6	41.8	34.7	25.1(ax)[b] 36.4(eq)[b]	28.5

[a] M3N, *N*-methylaziridine; M4N, *N*-methylazetidine; M5N, *N*-methylpyrrolidine; M6N, *N*-methylpiperidine; M7N, *N*-methylazepane.
[b] ax, methyl-axial conformer; eq, methyl-equatorial conformer (see Ref. [26]).

7.2. ICT activation energy and nitrogen inversion barrier

The increase of the ICT activation energy E_a in the series P7C-P3C (preceding section and Table 1) is attributed to the increase in activation energy for the configurational change of the amino nitrogen towards planarity. Such an increase of the amino nitrogen inversion barrier with decreasing ring size has been observed for the polymethyleneimines *N*-methylazepane (M7N) to *N*-methylaziridine (M3N) (see Table 2).

It follows from the oxidation potentials that M5N (0.68 V vs. SCE) is a better electron donor than M6N (0.80 V vs. SCE) [30]. Therefore, the smaller ICT efficiency of P5C as compared to P6C cannot easily be explained within the TICT context. This model treats the energetics of the CT state in a molecule such as DMABN as being determined by the redox potentials of the fully separated donor (dimethylamino) and acceptor (benzonitrile) moieties [1,2,9].

The results presented here mean that the change in the configuration of the amino nitrogen from partly pyramidal (sp^3) towards planar (sp^2) must be an important reaction coordinate in the ICT reaction of 4-aminobenzonitriles. The final CT state is therefore assumed to be planar. In support of this conclusion, it has been deduced from the absence of a correlation between the CT emission maxima and the redox potentials of the D and A subunits of the aminobenzonitriles that the amino and benzonitrile groups are strongly electronically coupled in the CT states of these compounds (see below and Ref. [9]).

7.3. ICT mechanism. $\Delta E(S_1,S_2)$ and configurational change of the amino nitrogen

From an analysis of absorption spectra and photostationary or time-resolved fluorescence data [3,4,9,11,16] it is concluded that two factors are of essential importance for the occurrence of an ICT reaction and dual fluorescence with aminobenzonitriles. Firstly, the energy gap $\Delta E(S_1,S_2)$ should be sufficiently small for efficient vibronic coupling: a solvent-induced pseudo-Jahn–Teller interaction leading to the final 'anomalous' CT state. Secondly, the energy barrier for the configurational change of the amino nitrogen from partly pyramidal [31] towards planar should be low enough to make this change possible within the time range set by the excited state reaction. This is concluded from the strong influence, discussed above, of ring size on ICT in the series P8C to P3C.

7.4. An experimental test of rotational isomerisation and electronic decoupling

The assumption of rotational isomerisation of the TICT model has been experimentally tested in two ways. In the first approach [1,2], the fluorescence of model compounds was investigated, in which the amino group either was forced to be already strongly twisted in the ground state by two ortho methyl groups (MMD) or was prevented from rotation by a chemical linkage to the phenyl group (NMCQ).

A second configurational test of the TICT hypothesis consists in a study designed to establish whether or not a (linear) correlation exists between the CT emission maximum $h\nu^{max}$ (CT) and the redox potentials of the amino (D) and benzonitrile (A) moieties [32]. These D and A groups were supposed to be electronically practically completely decoupled in the final CT state. The search for such a correlation is a logical consequence of the TICT hypothesis.

7.5. CT emission maximum and the redox potentials of the A and D subunits

In a CT system such as an intermolecular exciplex $^1(A^-D^+)$ the electronic stabilization of the CT state is largely determined by the difference between the redox potentials E_{ox} (D) and E_{red} (A) together with the Coulombic energy $C(A^-D^+)$, due to attraction between the ionic species A^- and D^+ at the distance prevalent in the exciplex [33]. Besides these Coulombic macroscopic factors, the intermolecular electronic coupling between A^- and D^+ also plays a role. The generally minor importance of these electronic factors can be deduced from the fact that the exciplex energy $E(A^-D^+)$ often indeed shows a linear correlation with the difference between the redox potentials of A and D (E_{ox} (D) − E_{red} (A)) [34].

Based on early photostationary experiments [33,34] with aromatic hydrocarbons (e.g. anthracene) and amines (*N*,*N*-diethylaniline), employing the temperature dependence of the exciplex/monomer fluorescence intensity ratio I'/I, a semiempirical correlation between the exciplex energy $E(A^-D^+)$ and the redox potentials of A and D was derived, the Weller equation (Eq. (2)):

$$E(A^-D^+) = E_{ox}(D) - E_{red}(A) + 0.15 \pm 0.10\ \text{eV} \qquad (2)$$

This equation with the numerical factor 0.15 is valid for an unpolar solvent such as n-hexane [33].

For the energy of the exciplex emission maximum $h\nu_{max}$ (CT) Eq. (3) holds (Fig. 8).

$$h\nu^{max}(CT) = E(A^-D^+) - \delta E_{rep} \qquad (3)$$

A relation between $h\nu^{max}$ (CT) and the redox potentials E_{ox} (D) and E_{red} (A) (Eq. (4)) is then obtained from Eqs. (2) and (3) (C is a constant).

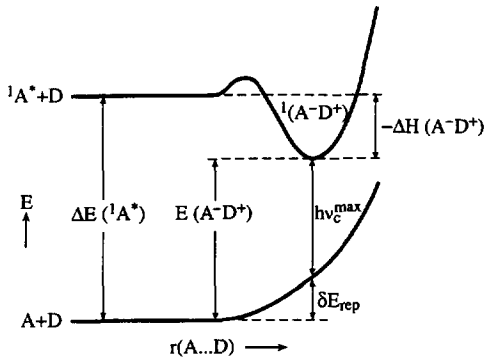

Fig. 8. Potential energy diagram for exciplex formation and fluorescence. From an electron acceptor in the singlet excited state $^1A^*$ and an electron donor D, the exciplex $^1(A^-D^+)$ is formed with a stabilisation enthalpy difference $\Delta H(A^-D^+)$. The Franck–Condon state reached after exciplex emission is destabilised with respect to the relaxed pair of ground state molecules (A + D) by the repulsion energy δE_{rep}.

$$h\nu^{max}(CT) = E_{ox}(D) - E_{red}(A) + C - \delta E_{rep} \quad (4)$$

It is clear from Eq. (4) that a linear correlation between $h\nu^{max}$ (CT) and the redox potentials of A and D is only to be expected when δE_{rep} has the same value for all exciplexes employed in the investigation. These considerations have been treated in more detail elsewhere [9].

7.6. Correlation of the CT emission maximum of aminobenzonitriles with the oxidation potential of the D subunit

A plot of the CT emission maxima $h\nu^{max}$ (CT) of a series of 4-aminobenzonitriles against the oxidation potential E_{ox} (D) of the amino group (Fig. 9(a)) shows that a correlation between these parameters does not exist. The same conclusion is drawn when $h\nu^{max}$ (CT) is plotted versus the vertical ionisation potential IP(D) of the donor subunit [9].

It is therefore concluded that there is no evidence for an electronic decoupling of the D and A subunits in the CT state of a dual fluorescent aminobenzonitrile, as required by the TICT hypothesis. A substantial electronic coupling in the CT state is in accord with the planar molecular configuration of this state that is assumed here on the basis of the influence on the ICT reaction of the ring size of the amino substituent in the compounds P3C–P8C (see above) [9].

7.7. Dual fluorescent bianthryls. Correlation of the CT emission maximum and redox potentials

The ICT process taking place in 9,9′-bianthryl (BA), in which the two anthryl groups act as electron donor and acceptor, has been considered to be mechanistically similar to that occurring with an aminobenzonitrile such as DMABN [2]. It is therefore of interest to see whether the CT emission maxima in the series BA, 10-cyano-9,9′-bianthryl (CBA) and 10,10′-dicyano-9,9′-bianthryl (DCBA) show a linear correlation with the redox potentials of the D and A anthryl moieties. Such a correlation indeed exists for BA, CBA and DCBA in toluene and acetonitrile [9] (see Fig. 9(b)).

Therefore, it is concluded that bianthryls are photophysically different from DMABN and are similar to exciplexes $^1(A^-D^+)$. The energetics of the CT reaction in bianthryls is mainly governed by the difference in free energy between the initial state $^1A^*A$ and the product CT state A^-A^+ and not by the magnitude of an energy gap $\Delta E(S_1,S_2)$ between two vibronically interacting excited states as in DMABN.

8. Donor/acceptor-substituted stilbenes

In D/A-substituted stilbenes such as trans-4-dimethylamino-4′-cyano-stilbene (DCS) an efficient ICT reaction occurs in the singlet excited state. This follows from the observation that the dipole moment strongly increases from $\mu_g = 7.0$ D in the ground state to around 22 D in the equilibrated S_1 state (see Table 3) [6]. This ICT process is accompanied by trans–cis isomerisation [35].

It has been a point of discussion, however, whether the final CT state of a stilbene such as DCS is reached directly by excitation from the ground state (with subsequent solute/

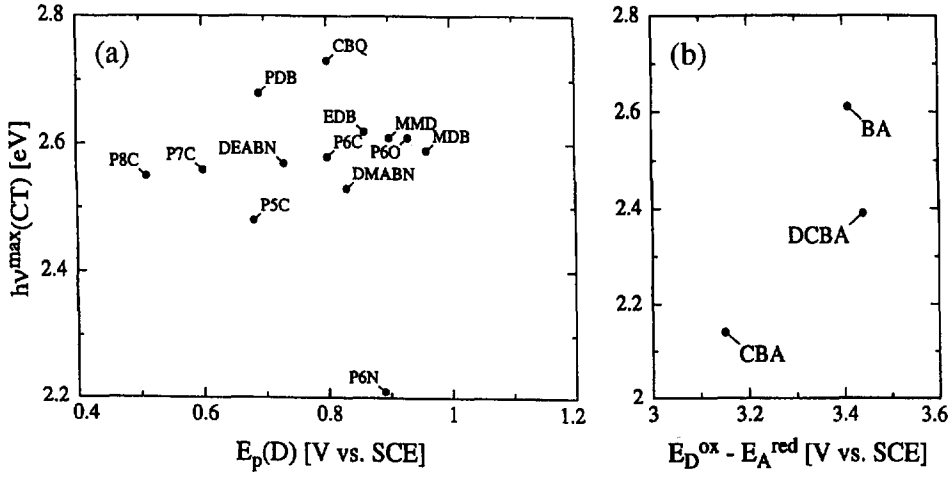

Fig. 9. Energy $h\nu^{max}$(CT) of the CT emission maximum in acetonitrile at 20 °C for (a) a series of 4-aminobenzonitriles (see Section 2) plotted against the peak oxidation potential E_p(D) of the N-methyl derivative of the amino substituent and for (b) 9,9-bianthryl (BA), 10-cyano-9,9-bianthryl (CBA) and 10,10′-dicyano-9,9-bianthryl (DCBA) plotted against the redox potential difference (E_D^{ox}–E_A^{red}) of the D and A anthryl groups.

Table 3
Fluorescence quantum yields Φ(LE) and Φ'(CT), fluorescence decay parameters (τ_1, τ_2, A), CT radiative rate constant k'_f and dipole moments for ground (μ_g) and CT state (μ_e(CT)) at 25 °C

	ΦE	'(CT)	τ_1 (ns)	τ_2 (ns)	A [b]	k'_f (10^6 s^{-1})	μ_g (D)	μ_e(CT) (D)
DCS	-	0.15	0.51[a]	–	–	290 [c]	7.0 [d]	22 [d]
ACS	-	0.14	0.47[a]	–	–	290 [c]	(7.0)	>23 [e]
DMABN	0.001	0.025	(3.12) [f]	0.006[f]	(>10) [f]	–	6.6	16 [g]
P4C	0.05	0.015	2.97[a]	0.269[a]	6.2	5.4 [h]	6.5	17.5 [i]

[a] Ref. [11].
[b] $A = A_{12}/A_{11}$ derived from the LE fluorescence decay $i(\leq) = A_{12}e^{-t/\tau_2} + A_{11}e^{-t/\tau_1}$.
[c] From $k'_f = \Phi'(CT)/\tau_1$.
[d] Ref. [6].
[e] From solvatochromic measurements relative to DCS. This difference in dipole moment $\Delta\mu$ was determined via the solvatochromic method by plotting the fluorescence maxima $h\nu^{max}$(CT) of ACS in a variety of solvents spanning the polarity scale against those of DCS in the same media. From the larger value ($\Delta\mu = 17$ D) measured for the difference in dipole moment between the ground and CT state of ACS as compared with DCS (Table 3), it follows that the azetidinyl group has somewhat stronger donor properties than the dimethylamino substituent (Refs. [6](b) [39]).
[f] Ref. [40] long decay time τ_1 mainly due to photochemical products.
[g] Ref. [4].
[h] Derived from $\Phi'(CT)/\Phi(LE)$ and the rate parameters of Scheme 1 (Ref. [3,13]).
[i] Ref. [13].

solvent equilibration) or that an LE state is primarily formed as a CT precursor [36]. From the single-exponential fluorescence decays of DCS in a variety of solvents such as diethyl ether and acetonitrile down to low temperatures (see Fig. 10) it is concluded that an LE precursor cannot be detected within the time resolution of our SPC equipment [6](b) [11].

As established previously [9,11,22], the replacement of the dimethylamino substituent of DMABN by an azetidinyl

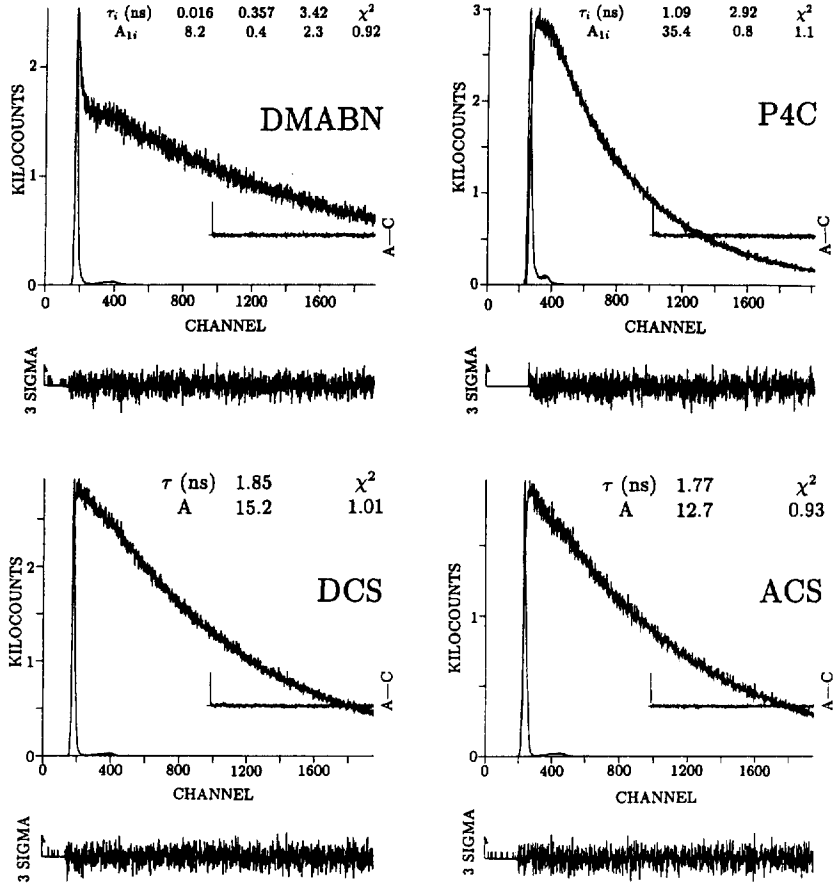

Fig. 10. Fluorescence response functions of (top) the LE emission of 4-(dimethylamino)benzonitrile (DMABN) and 4-(*N*-azetidinyl)benzonitrile (P4C) and (bottom) the CT fluorescence of 4-dimethylamino-4′-cyano-stilbene (DCS) and 4-azetidinyl-4′-cyano-stilbene (ACS) in acetonitrile at 25 °C. The decay times (τ_i) and their preexponential factors A_{1i} (LE) and A are given. See Fig. 1.

group (giving P4C) strongly slows down the ICT reaction (see Fig. 6). It was therefore of interest to see whether with trans-4-azetidinyl-4′-cyano-stilbene (ACS) an LE emission could be observed next to the CT band. This is not the case. The fluorescence spectra of ACS in, for example, diethyl ether and acetonitrile [11] are practically identical with those of DCS, giving no indication of the presence of dual emission. In addition, the difference $\Delta\mu$ between the ground and excited state dipole moments, the fluorescence quantum yields and the decay times of the two molecules are practically identical (see Table 3). Further, the fluorescence decays of both molecules are single exponential in acetonitrile at −40 °C (Fig. 10) as well as at 20 °C [11], which means that even at low temperatures there is no evidence for an LE state as precursor for the equilibrated CT state within a time range of 5–10 ps.

A change in the configuration of the amino nitrogen is clearly not an important reaction coordinate in the ICT process of DCS and ACS, indicating that the ICT pathway followed by these D/A-substituted stilbenes is different from that taken by DMABN.

8.1. D/A-substituted naphthalenes

To test the generality of the conclusion reached above for the aminobenzonitriles that the ICT reaction is primarily controlled by the energy gap $\Delta E(S_1,S_2)$, the two isomeric D/A-substituted naphthalenes 1-dimethylamino-4-cyanonaphthalene (1,4-DCN) and 2-dimethylamino-6-cyanonaphthalene (2,6-DCN) are investigated. In the parent molecule naphthalene, the lowest singlet excited state S_1 is of ^1L_b character and its transition dipole moment is oriented along the long molecular axis, whereas the S_2 state is of ^1L_a nature and is short-axis polarised [37]. Hence, substituents in the short molecular axis as in 1,4-DCN mainly stabilise the $S_2(^1L_a)$ state and thereby decrease the $\Delta E(S_1,S_2)$ energy gap, which will strongly enhance the vibronic coupling between the ^1L_a and ^1L_b parent states and, in addition, with various CT states. With 2,6-DCN, in contrast, the D/A substituents stabilise the lower long-axis polarised $S_1(^1L_b)$ state, leading to a relatively large value for $\Delta E(S_1,S_2)$. These different substituent effects can be seen from the absorption spectra of 1,4-DCN and 2,6-DCN (Fig. 11), with a broad single lowest-energy absorption band in the case of 1,4-DCN and two separate absorption bands with 2,6-DCN.

8.2. Dual fluorescence with 1,4-DCN. LE emission with 2,6-DCN

With 1,4-DCN in acetonitrile dual fluorescence (LE and CT) is observed, whereas only LE emission is found in the case of 2,6-DCN (Fig. 11). These observations indicate that also for the D/A-substituted naphthalenes 1,4-DCN and 2,6-DCN, the occurrence of ICT and dual fluorescence is determined by the magnitude of the energy gap $\Delta E(S_1,S_2)$, showing the general character of the ICT mechanism treated above.

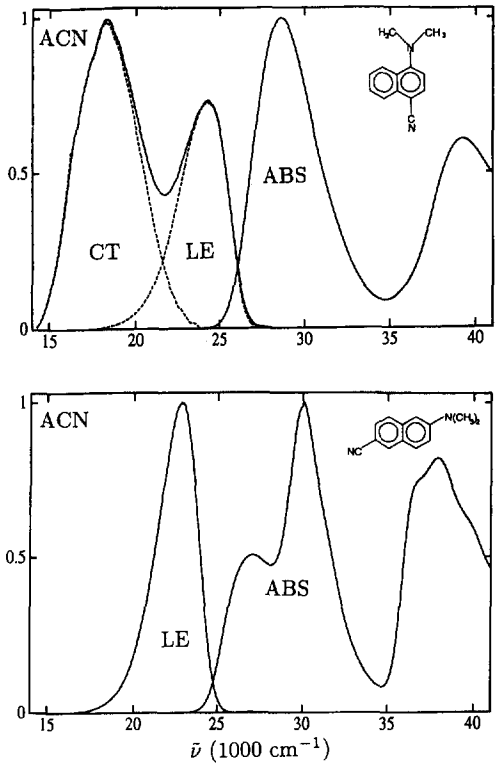

Fig. 11. Fluorescence and absorption spectra of 1-dimethylamino-4-cyanonaphthalene (1,4-DCN), above, and 2-dimethylamino-6-cyanonaphthalene (2,6-DCN), below, in acetonitrile at 25 °C, see text.

9. Conclusion

From the experimental results discussed here it is concluded that two requirements have to be fulfilled for the occurrence of ICT and dual fluorescence in aminobenzonitriles: (a) a sufficiently small energy gap $\Delta E(S_1,S_2)$ between the two vibronically interacting lowest excited states ($S_1(^1L_b)$ and $S_2(^1L_a,CT)$ in the case of DMABN), leading to a solvent polarity induced pseudo-Jahn–Teller coupling; and (b) an energetically possible change from the partly pyramidal configuration of the amino nitrogen in the ground state to the planar structure of the final CT state. The occurrence of ICT in the D/A-substituted naphthalenes 1,4-DCN and its absence with 2,6-DCN is likewise governed by the magnitude of the energy gap $\Delta E(S_1,S_2)$.

It is concluded from the absence of a linear correlation between the CT emission maximum $h\nu^{max}$ (CT) and the redox potentials of the D and A subunits of a series of 4-aminobenzonitriles, that the D and A subgroups are not electronically decoupled in the final CT state, as postulated in the TICT model. Such a linear correlation does occur, however, for the three 9,9′-bianthryls BA, CBA and DCBA, showing that the factors governing the ICT reaction in these bianthryls are fundamentally different from those determining the ICT processes in the 4-aminobenzonitriles.

With the D/A-substituted stilbenes DCS and ACS, an LE precursor could not be observed within a time resolution of 5–10 ps (acetonitrile, −40 °C). The presence of a 4-azeti-

dinyl electron donor group in ACS does not reduce the ICT efficiency as compared to DCS, in contrast to what has been observed with P4C relative to DMABN, which shows that a change in the configuration of the amino group is not an important reaction coordinate in these stilbenes.

The photophysical behaviour of a dual fluorescent 4-aminobenzonitrile such as DMABN is, as compared with other molecules undergoing ICT, unusually sensitive to relatively minor changes in molecular structure. An example is the disappearance of ICT in MABN and the dicyano compounds 3,4-DCDMA and 3,5-DCDMA. This sensitivity is interpreted as an indication of a resonance phenomenon between two neighbouring excited states, very different from what is encountered in the case of inter- and intramolecular exciplexes, 9,9′-bianthryl, 9-(4-N,N-dimethylanilino)-anthracene [38] and DCS, for which small structural changes lead to small effects on the ICT reaction. These latter systems are governed by the magnitude of the difference in free energy ΔG between the LE and CT states, which is largely determined by the macroscopic Coulombic energy that is set free by the increased charge separation in the excited state. In contrast to DMABN and related molecules, the specific nature of the different molecular states S_n does not play a significant role. The special photophysical aspects of DMABN should be taken into account in theoretical treatments of this molecule.

Acknowledgements

Thanks are due to Prof. W. Baumann, Dr. Wortmann and Dr. N. Detzer, Mainz, for putting CBA and CBQ at our disposal. The generous financial support received from the Volkswagen Foundation (Project "Intra-and intermolecular electron transfer") is gratefully acknowledged.

References

[1] Z.R. Grabowski, K. Rotkiewcz, A. Siemiarczuk, D.J. Cowley and W. Baumann, *Nouv. J. Chim., 3* (1979) 443.
[2] E. Lippert, W. Rettig, V. Bonačič-Koutecký, F. Heisel and J.A. Miehé, *Adv. Chem. Phys., 68* (1987) 1.
[3] U. Leinhos, W. Kühnle and K.A. Zachariasse, *J. Phys. Chem., 95* (1991) 2013.
[4] W. Schuddeboom, S.A. Jonker, J.M. Warman, U. Leinhos, W. Kühnle and K.A. Zachariasse, *J. Phys. Chem., 96* (1992) 10809.
[5] (a) PCMODEL, Serena Software, Bloomington, IN. (b) J.J. Gajewski, K.E. Gilbert and J. McKelvey, in D. Liotta (ed.), *Advances in Molecular Modeling*, JAI Press, Greenwich, CN, 1990, Vol. II, p.65.
[6] I. Gryczyński, D. Gloyna and A. Kawski, *Z. Naturforsch., 35A* (1980) 777. (b) Yu.V. Il'ichev, W. Kühnle and K.A. Zachariasse, *Chem. Phys.*, in press.
[7] E. Lippert, W. Lüder, F. Moll, H. Nagele, H. Boos, H. Prigge and I. Siebold-Blankenstein, *Angew. Chem., 73* (1961) 695.
[8] (a) K. Rotkiewicz, K.H. Grellmann and Z.R. Grabowski, *Chem. Phys. Lett., 21* (1973) 212. (b) O.S. Khalil, R. Hofeldt and S.P. McGlynn, *Chem. Phys. Lett., 35* (1975) 172. (c) E.M. Kosower and H. Dodiuk, *J. Am. Chem. Soc., 98* (1976) 924. (d) R.J. Visser, C.A.G.O. Varma, *J. Chem. Soc., Faraday Trans. 2, 76* (1980) 453. (e) C. Cazeau-Dubroca, S. Ait Lyazidi, P. Cambou, A. Peirigua, Ph. Cazeau and M. Pesquer, *J. Phys. Chem., 93* (1989) 2347.
[9] Th. von der Haar, A. Hebecker, Yu. Il'ichev, Y.-B. Jiang, W. Kühnle and K.A. Zachariasse, *Rec. Trav. Chim. Pays-Bas, 114* (1995) 430.
[10] (a) G. Striker, in M. Bouchy (ed.), *Deconvolution and Reconvolution of Analytical Signals*, University Press, Nancy, 1982, p. 329. (b) K.A. Zachariasse, G. Duveneck, W. Kühnle, P. Reynders and G. Striker, *Chem. Phys. Lett., 133* (1987) 390.
[11] Th. von der Haar, A. Hebecker, Yu. Il'ichev, W. Kühnle and K.A. Zachariasse, *Fast Elementary Processes in Chemical and Biological Systems*, AIP Conference Proceedings 364, Lille, France, 1995, p. 295.
[12] A. Hebecker, Th. von der Haar and K.A. Zachariasse, in preparation.
[13] Th. von der Haar, *Ph.D. Thesis*, University Göttingen, 1994.
[14] U. Leinhos, *Ph.D. Thesis*, University Göttingen, 1991.
[15] (a) T.J. Kang, W. Jarzeba and P.F. Barbara, *Chem. Phys., 149* (1990) 81. (b) J.-B. Jiang, Yu. Il'ichev and K.A. Zachariasse, in preparation.
[16] K.A. Zachariasse, Th. von der Haar, A. Hebecker, U. Leinhos and W. Kühnle, *Pure Appl. Chem., 65* (1993) 1745.
[17] (a) J.R. Platt, *J. Chem. Phys., 17* (1949) 484. (b) J.N. Murrell, *The Theory of the Electronic Spectra of Organic Molecules*, Methuen, London, 1963.
[18] J. Herbich, K. Rotkiewicz, J. Waluk, B. Andresen and E.W. Thulstrup, *Chem. Phys., 138* (1989) 105.
[19] W. Baumann, Z. Nagy, A.K. Maiti, H. Reis, S.V. Rodrigues and N. Detzer, *Dynamics and Mechanisms of Photoinduced Electron Transfer and Related Phenomena*, N. Mataga, T. Okada and H. Masuhara (eds.), North–Holland, Amsterdam, 1992, p. 211.
[20] M. Grobys, Yu. Il'ichev and K.A. Zachariasse, in preparation.
[21] T. Kobayashi, M. Futakami and O. Kajimoto, *Chem. Phys. Lett., 141* (1987) 450.
[22] K.A. Zachariasse, Th. von der Haar, U. Leinhos and W. Kühnle, *J. Inf. Rec. Mater., 21* (1994) 501.
[23] M.C.C. de Lange, D. Thorn Leeson, K.A.B. van Kuijk, A.H. Huizer and C.A.G.O. Varma, *Chem. Phys., 177* (1993) 243.
[24] A. Kummer, W. Kühnle and K.A. Zachariasse, in preparation.
[25] A. Rieker and H. Kessler, *Tetrahedron, 23* (1967) 3723.
[26] M. Oki, *Applications of Dynamic NMR Spectroscopy to Organic Chemistry*, VCH, Weinheim, 1985.
[27] J. Dobkowski, Z.R. Grabowski, J. Jasny and Z. Zielinski, *Acta Phys. Polon. A, 88* (1995) 455.
[28] (a) P.H. Rieger, I. Bernal, W.H. Reinmuth and G.K. Fraenkel, *J. Am. Chem. Soc., 85* (1963) 683. (b) D. van der Meer, *Ph.D. Thesis*, Technical University Twente, The Netherlands, 1970. (c) N. Koizumi and S. Aoyagui, *J. Electroanal. Chem., 139* (1982) 69.
[29] W. Rettig, *Ber. Bunsenges. Phys. Chem., 95* (1991) 259.
[30] J.R. Lindsay Smith and D. Masheder, *J. Chem. Soc., Perkin Trans., 2* (1976) 47.
[31] A. Heine, R. Herbst-Irmer, D. Stalke, W. Kühnle and K.A. Zachariasse, *Acta Crystallogr., B50* (1994) 363.
[32] Z.R. Grabowski and J. Dobkowski, *Pure Appl. Chem., 55* (1983) 245.
[33] (a) A. Weller, *Z. Phys. Chem., 133* (1982) 93. (b) A. Weller, *Z. Phys. Chem., 130* (1982) 129.
[34] A. Weller, in M. Gordon and W.R. Ware (eds.), *The Exciplex*, Academic, New York, 1975, p. 23.
[35] H. Görner and H.J. Kuhn, *Adv. Photochem., 19* (1995) 1.
[36] (a) R. Lapouyade, K. Czeschka, W. Majenz, W. Rettig, E. Gilabert and C. Rullière, *J. Phys. Chem., 96* (1992) 9643. (b) T. Gustavsson, G. Baldacchino, J.-C. Mialocq and S. Pommeret, *Chem. Phys. Lett., 236* (1995) 587.
[37] J.B. Birks, *Photophysics of Aromatic Molecules*, Wiley, London, 1970.
[38] P.F. Barbara and W. Jarzeba, *Adv. Photochem., 15* (1990) 1.
[39] A. Kawski, B. Ostrowska and M. Stoń, *Z. Naturforsch., 36A* (1981) 999.
[40] P. Geggier and K.A. Zachariasse, unpublished results.